

# Analysis of Advanced Metering over a Wide Area Cellular Network

Michael R. Souryal and Nada Golmie  
National Institute of Standards and Technology  
Emerging and Mobile Network Technologies Group  
Gaithersburg, Maryland, USA

**Abstract**—This paper presents a framework for analysis of the coverage and capacity of advanced metering over a wide area cellular network. The coverage analysis predicts the maximum cell size subject to an outage criterion, and the capacity analysis predicts the maximum rate at which a smart meter can send and receive messages over the wide area portion of the network. The framework permits quantification of the tradeoff between coverage and capacity, as well as the impact of variables associated with the radio frequency environment, system configuration, and network utilization. The framework is illustrated through an example analysis of Long Term Evolution, a pre-fourth-generation cellular technology. Results suggest that the network is coverage-limited rather than capacity-limited for the meter reading use case, and it quantifies the excess capacity available for other uses and/or other entities sharing the network.

## I. INTRODUCTION

Among the challenges of smart metering is communicating with a large number of meters over a wide service territory in an efficient, scalable, and manageable manner. While one may consider wired or wireless technologies—the relative merits of which are summarized in [1] in the context of the smart grid—this paper looks at a class of wireless solutions. A range of wireless technologies is described in [2], including local area, metropolitan area, wide area, and mesh technologies, along with the opportunities and challenges associated with their use in the smart grid. In [3], we presented a methodology for quantitative performance evaluation of wireless deployments, and we applied the methodology to the evaluation of a neighborhood area metering network utilizing the IEEE 802.11 wireless local area network standard.

In this paper, we present a framework for analyzing the performance of an advanced metering application operating over a wide area cellular network. The framework consists of two major components. A coverage analysis predicts the maximum cell size subject to an outage criterion, and a capacity analysis predicts the maximum rate at which a smart meter can send and receive messages over the wide area network (WAN). Both components utilize a conventional channel propagation model that approximates the attenuation of the radio frequency (RF)

signal with distance as well as the variability of the received signal strength due to shadowing. The capacity analysis also accounts for inter-sector interference from neighboring sectors as a function of their utilization. The analysis permits us to quantify the tradeoff between coverage and capacity, as well as the impact of variables such as the propagation environment, system characteristics (e.g., bandwidth, antenna radiation pattern), and network utilization.

We illustrate the framework through an example analysis of 3rd Generation Partnership Project (3GPP) Long Term Evolution (LTE), a pre-fourth-generation cellular technology that some U.S. carriers have chosen for nationwide deployment. Our analysis suggests that the WAN is coverage-limited rather than capacity-limited for the meter reading use case, and it quantifies the excess capacity available for other uses and/or other entities sharing the network.

The remainder of this paper is organized as follows. Section II states the assumptions with respect to the application traffic, radio access network, and RF propagation model. Section III describes the approach to the coverage analysis and presents quantitative results for typical urban and rural environments. Section IV analyzes the communication capacity of the smart meter in both the uplink and downlink. Finally, Section V summarizes the key observations and conclusions of the analysis.

## II. SYSTEM MODEL

### A. Advanced Metering Architecture and Application Traffic

For the purpose of this analysis, we assume that centralized metering operations systems communicate with two-way meters at the customer premises over a wide area network, possibly using neighborhood area networks, as well. A metering headend has a connection (not necessarily wireless) to the core network and utilizes the radio access network to communicate with a number of data aggregation points (DAPs) (see Fig. 1). The core network and access network comprise the wide area network. The DAPs, in turn, communicate with the meters through neighborhood area networks, likely using a different technology from that used on the wide area access network.

An alternative architecture is for the WAN interface to reside in the meters rather than in the DAPs, bypassing the DAPs and providing a direct connection between the headend and the meters. This paper considers the performance of the wide

Certain commercial equipment, instruments, or materials are identified in this paper in order to specify the experimental procedure adequately. Such identification is not intended to imply recommendation or endorsement by the National Institute of Standards and Technology, nor is it intended to imply that the materials or equipment identified are necessarily the best available for the purpose.

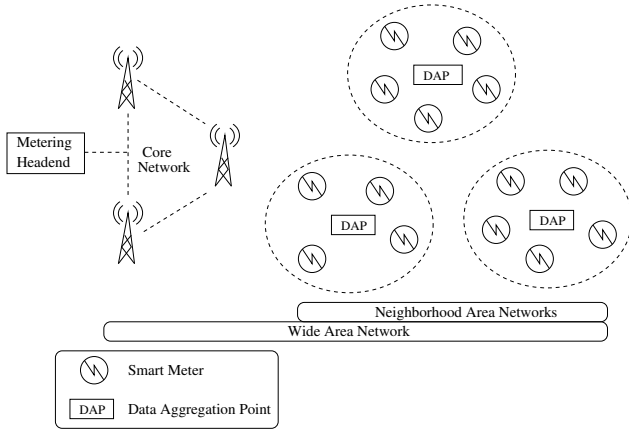


Fig. 1. Metering network topology

TABLE I  
LTE SYSTEM PARAMETERS

Base Station (eNodeB)	Transmission Power	43 dBm
	Peak Antenna Gain	12 dBi (urban) 15 dBi (rural)
	Noise Figure	5 dB
Terminal (UE)	Transmission Power	24 dBm
	Antenna Gain (omnidirectional)	0 dBi
	Noise Figure	9 dB

area network portion of the architecture, and applies equally whether the WAN link terminates at the DAP or at the meter. In the case of the first architecture, the analysis neglects any aggregation efficiencies that may exist at the DAP.

Application traffic is present both on the downlink from the headend to the DAPs/meters and on the uplink from the DAPs/meters to the headend. The example analysis for the meter reading and service switch use cases presented in [4, Section 3.6] concludes that a total of 152 messages per 1000 meters per day are transmitted on the downlink, with each message being 25 bytes in length. On the uplink, the message rates and sizes vary, with the average rate being close to 7.9 messages per meter per day and the average size being 2133 bytes. The analysis below assumes these average application message sizes plus 42 bytes of additional network and transport layer overhead per message.

### B. Radio Access Network

The radio access network is an LTE system operating in a frequency division duplex (FDD) mode at 700 MHz. The bandwidth is assumed to be 5 MHz in each direction. Additional LTE system parameters are taken from [5] and are summarized in Table I.

We assume cells are sectorized into three 120° sectors. Each sector antenna has a directive radiation pattern given in decibels as a function of the azimuth ( $\theta$ ) in degrees by [5]

$$A(\theta) = -\min \left[ 12 \left( \frac{\theta}{65} \right)^2, 20 \right]; -180 \leq \theta \leq 180 \quad (1)$$

where  $\theta = 0^\circ$  is the boresight angle. While LTE supports multi-antenna transmission schemes, including transmit diversity and spatial multiplexing, the analysis below conservatively assumes the use of single-input/single-output antennas.

LTE specifies 29 modulation-coding schemes (MCSs) that vary in spectral efficiency and robustness to channel errors. The analysis assumes channel-dependent adaptation of the modulation-coding scheme (MCS) whereby a link uses the highest-order MCS supported by the link's received signal-to-noise ratio (SNR).

### C. Channel Propagation Model

The channel propagation model follows the recommendations in [5] for macro cells in urban and rural areas. The median path loss as a function of distance is given therein for an urban area in dB as

$$L_{\text{urban}}(d) = 40(1 - 4 \times 10^{-3} h_{b,\Delta}) \log_{10}(d) - 18 \log_{10}(h_{b,\Delta}) + 21 \log_{10}(f_c) + 80 \quad (2)$$

where  $d$  is the base station-user equipment (UE) separation distance in kilometers,  $f_c$  is the carrier frequency in megahertz, and  $h_{b,\Delta}$  is the base station antenna height in meters above the average rooftop level. For  $f_c = 700$  MHz and  $h_{b,\Delta} = 15$  m, (2) simplifies to

$$L_{\text{urban}}(d) = [37.6 \log_{10}(d) + 118.6] \text{ dB}.$$

The median path loss for a rural area is based on the Hata model and is given in dB by

$$L_{\text{rural}}(d) = 69.55 + 26.16 \log_{10}(f_c) - 13.82 \log_{10}(h_b) + [44.9 - 6.55 \log_{10}(h_b)] \log_{10}(d) - 4.78 (\log_{10} f_c)^2 + 18.33 \log_{10}(f_c) - 40.94 \quad (3)$$

where  $h_b$  is the base station antenna height above ground in meters. For  $f_c = 700$  MHz and  $h_b = 45$  m, (3) reduces to

$$L_{\text{rural}}(d) = [34.1 \log_{10}(d) + 93.6] \text{ dB}.$$

In addition to the deterministic path loss versus distance, there is a random component,  $X_s$ , that models shadowing (or slow fading) with a lognormal distribution having zero mean and standard deviation  $\sigma_s$  in the log domain. In outdoor environments,  $\sigma_s$  typically ranges from 6 dB to 10 dB.

## III. COVERAGE ANALYSIS

The coverage analysis aims to determine the maximum distance the UE can be located from the base station, neglecting capacity constraints. The maximum transmitter-receiver distance is typically defined in terms of a criterion such as a maximum outage probability at a specified data rate.

We consider the coverage limit in terms of the maximum cell radius of a hexagonal cell (base station-to-corner distance) such that the outage probability at the cell edge is below an outage threshold. The outage probability is the probability that the received SNR, modeled as random due to shadowing, is below the SNR threshold,  $\gamma_0$ , that corresponds to the minimum

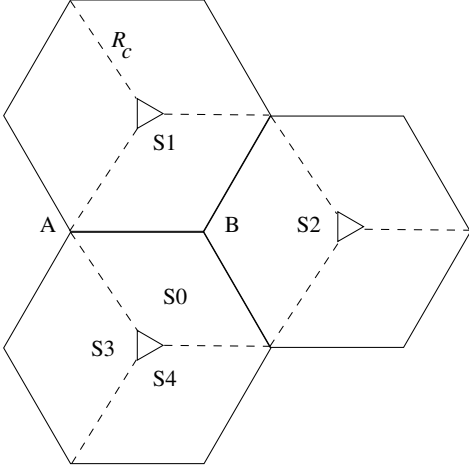


Fig. 2. A subset of three hexagonal cells

SNR required to support a given modulation-coding scheme or data rate.

Since the sector antenna gain varies with the azimuth, the outage probability varies along the cell edge. We therefore use the average outage probability along the cell edge as the metric, evaluated as

$$P_{\text{out}}(R_c) = \frac{1}{R_c} \int_A^B \Pr[\text{SNR}(s) \leq \gamma_0] ds \quad (4)$$

where the line integral is along an edge of a hexagonal cell with center-to-corner distance  $R_c$  (e.g., edge  $\overline{AB}$  in Fig. 2). The maximum cell radius is the largest  $R_c$  that satisfies

$$P_{\text{out}}(R_c) \leq P_{\text{out}}^*$$

where  $P_{\text{out}}^*$  is the maximum tolerable outage probability.

Using the system model in Section II, when the UE is at distance  $d$  and azimuth  $\theta$  from its sector antenna, the SNR in dB is given by

$$\text{SNR}(d, \theta) = P_{\text{rx}}(d, \theta) - 10 \log_{10}(kTB) - F \quad (5)$$

where  $P_{\text{rx}}(d, \theta)$  is the received power (dBm),  $k$  is Boltzmann's constant,  $T$  is the receiver noise temperature (Kelvin),  $B$  is the noise bandwidth (Hz), and  $F$  is the receiver's noise figure (dB).

The received power, in turn, is given by

$$P_{\text{rx}}(d, \theta) = P_{\text{tx}} + G_{\text{tx}} + A(\theta) - L(d) + G_{\text{rx}} + X_s \quad (6)$$

where  $P_{\text{tx}}$  is the transmission power (dBm),  $G_{\text{tx}}$  and  $G_{\text{rx}}$  are the transmitter and receiver peak antenna gains (dBi),  $A(\theta)$  is the sector antenna radiation pattern (1),  $L(d)$  is the deterministic path loss as a function of distance (e.g., (2) or (3)), and  $X_s$  is a zero-mean normal random variable with standard deviation  $\sigma_s$  (dB) representing shadowing. Since the only random component of the SNR is  $X_s$ , the SNR is also a normal random variable and the integrand of (4) can be expressed in terms of the error function:

$$\Pr[\text{SNR}(d, \theta) \leq \gamma_0] = \frac{1}{2} + \frac{1}{2} \text{erf} \left( \frac{\gamma_0 - \overline{\text{SNR}}(d, \theta)}{\sigma_s \sqrt{2}} \right) \quad (7)$$

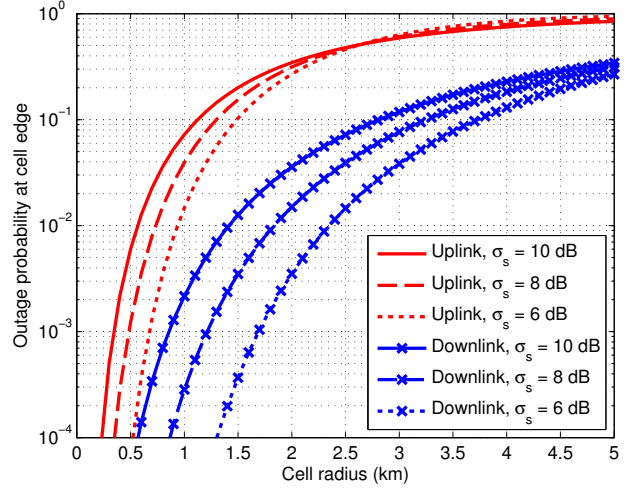


Fig. 3. Cell edge outage probability in urban environment

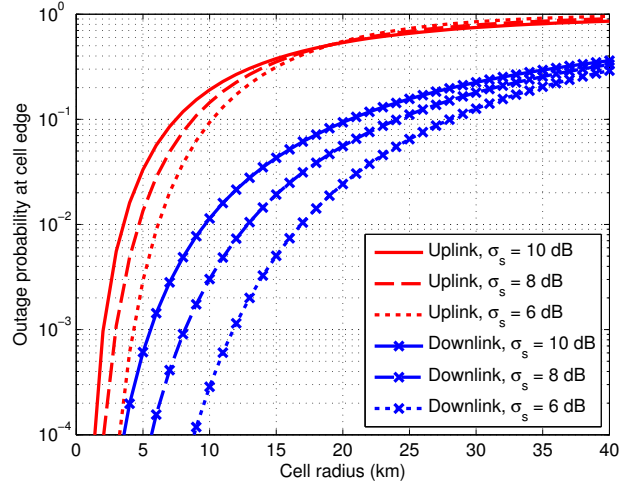


Fig. 4. Cell edge outage probability in rural environment

where from (5) and (6)  $\overline{\text{SNR}}(d, \theta)$  is the mean SNR in dB given by

$$\overline{\text{SNR}}(d, \theta) = P_{\text{tx}} + G_{\text{tx}} + A(\theta) - L(d) + G_{\text{rx}} - 10 \log_{10}(kTB) - F.$$

Figures 3 and 4 plot the average outage probability at the cell edge (4) versus the cell radius  $R_c$  in the urban and rural environments, respectively, as defined in Section II-C. We generated these curves assuming an SNR threshold of  $\gamma_0 = 2.4$  dB, the minimum SNR required by MCS 0. Both uplink and downlink outage probabilities are shown, and in each case three curves are plotted, for lognormal shadowing standard deviations of 6 dB, 8 dB, and 10 dB. As expected, the cell range is limited by the uplink outage probability, since the transmission power is lower on the uplink than on the downlink.

The outage probability considered herein assumes the UE has only one sector to choose from. In practice, the UE may have multiple sectors to choose from, especially near the cell

edge. Taking sector diversity into account, the actual outage probability will be less than that calculated above.

Assuming conservatively that a UE at the cell edge has only two sectors to choose from, and assuming liberally that the shadow fading is independent between the two links, the actual outage probability can be approximated as  $P_{\text{out}}^2$ ; in other words, outage with two-sector diversity occurs when the UE is in outage with respect to both sectors simultaneously. Thus, if the maximum tolerable outage with sector diversity is  $P_{\text{out}}^*$ , then the maximum  $R_c$  is that which yields an outage probability without sector diversity of  $\sqrt{P_{\text{out}}^*}$ .

For an outage probability  $P_{\text{out}}^*$  of 5 % (i.e.,  $\sqrt{P_{\text{out}}^*} = 0.22$ ) and  $\sigma_s = 8$  dB, the corresponding uplink outage curves in Figs. 3 and 4 indicate a maximum cell radius of 1.7 km in the urban environment and 11 km in the rural environment.

#### IV. CAPACITY ANALYSIS

##### A. Overview

The objective of the capacity analysis is to calculate the maximum achievable message rate of each smart meter. We base this calculation on the minimum number of LTE resource blocks needed in total to allow each smart meter in the sector to send a message to the headend on the uplink or receive a message from the headend on the downlink. Together with the rate at which resource blocks are transmitted (a function of the system bandwidth), the required number of resource blocks determines the minimum time interval,  $\tau_{\min}$ , needed for a round of messages to be sent or received by the smart meters. The inverse of  $\tau_{\min}$  yields the maximum message rate per smart meter. We calculate these quantities separately for the uplink and downlink.

The number of resource blocks required to send or receive a message on a given link depends on the MCS that can be supported on that link. The MCS, in turn, depends on the received signal-to-interference-and-noise ratio (SINR). The SINR, like the SNR used earlier in the coverage analysis, is a random variable. Here, the randomness is due to shadowing, the location of the UE (DAP or smart meter) in the sector, and the interference generated by other sectors. As a consequence, the MCS, adapted to the SINR of the link, also is a random variable.

We use the distribution of the SINR to compute the probability mass function (pmf) of the link-adapted MCS. With this pmf, along with the block size of each MCS, we calculate the average number of resource blocks required by all the links in the sector.

##### B. Capacity per Smart Meter

Let  $B_i$  be the payload size in bits of a resource block transmitted with MCS  $i$ , and let  $L$  represent the length of the message including overhead from higher layers. Then, the number of resource blocks required to send the message with MCS  $i$  is

$$N_i = \left\lceil \frac{L}{B_i} \right\rceil$$

where  $\lceil x \rceil$  is the smallest integer greater than or equal to  $x$ .

Furthermore, let  $K$  be the average number of smart meters in the sector. Then, the average number of resource blocks required for all  $K$  smart meters to send/receive a round of messages is

$$N_{\text{rb}} = K \sum_{i=0}^{28} N_i P_{\text{mcs},i} \quad (8)$$

where  $P_{\text{mcs},i}$  is the probability that a link uses MCS  $i$ . The average number of smart meters,  $K$ , is calculated by multiplying the geographic density of smart meters,  $\rho$ , by the area of the sector, assuming a three-sector hexagonal cell:

$$K = \frac{\sqrt{3}}{2} R_c^2 \rho.$$

The minimum time interval to transmit  $N_{\text{rb}}$  resource blocks is

$$\tau_{\min} = \frac{N_{\text{rb}}}{R_{\text{rb}}}$$

where  $R_{\text{rb}}$  is the rate at which resource blocks can be sent and depends on the system bandwidth. For example, for a bandwidth of 5 MHz, the resource block rate is  $R_{\text{rb}} = 25 \times 10^3$  resource blocks per second (25 resource blocks per sub-frame  $\times$  1000 sub-frames per second).

Finally, since each smart meter can send or receive a message at most every  $\tau_{\min}$  seconds, the maximum message rate per smart meter is

$$C_{\text{sm}} = \frac{1}{\tau_{\min}}.$$

##### C. MCS Probabilities

The smart meter capacity is a function of the MCS pmf through (8). If we denote as  $\gamma_i$  the minimum SINR needed to reliably transmit a symbol with MCS  $i$ , then the MCS pmf is given by

$$\begin{aligned} P_{\text{mcs},i} &= \Pr[\gamma_i \leq \text{SINR} < \gamma_{i+1}] \quad ; \quad 0 \leq i \leq 28 \\ &= \Pr[\text{SINR} < \gamma_{i+1}] - \Pr[\text{SINR} < \gamma_i] \end{aligned}$$

where  $\Pr[\text{SINR} < \gamma_{29}] \equiv 1$ .

On the downlink, the SINR in dB at UE location  $(d_0, \theta_0)$  with respect to its sector antenna is

$$\text{SINR}_{\text{dl}}(d_0, \theta_0, \mathcal{I}) = \text{SNR}(d_0, \theta_0) - \sum_{j \in \mathcal{I}} P_{\text{rx}}(d_j, \theta_j) \quad (9)$$

where the summation represents the total interference:  $\mathcal{I}$  is the set of sectors which are transmitting in the same time-frequency resource as the link of interest, and  $(d_j, \theta_j)$  is the location of the UE with respect to sector  $j$ .

The distribution of the SINR is obtained by averaging the conditional distribution of (9) over the location of the UE and over the set of active interferers:

$$\Pr[\text{SINR}_{\text{dl}} \leq \gamma] = E_{d_0, \theta_0, \mathcal{I}} \{ \Pr[\text{SINR}_{\text{dl}}(d_0, \theta_0, \mathcal{I}) \leq \gamma] \}. \quad (10)$$

We compute the expectation over  $d_0$  and  $\theta_0$  assuming that the location of the UE is uniformly distributed in the sector. We compute the expectation over  $\mathcal{I}$  assuming that each sector

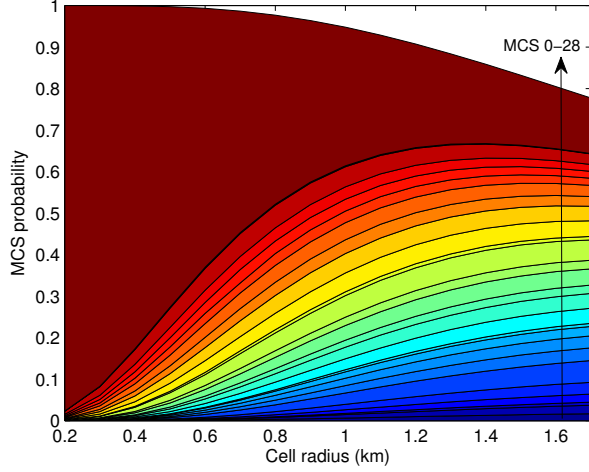


Fig. 5. Uplink MCS probabilities in urban environment with 8 dB shadowing and 6 dB uplink noise rise

transmits in the resource block of interest with a given probability independently of other sectors. This probability of transmission is parameterized below as the downlink sector utilization,  $v$ .

The conditional probability inside the expectation on the right-hand-side of (10) is evaluated as in (7) where, for tractability, we only account for the lognormal shadowing on the link from the desired sector and neglect shadowing on the links from the interfering sectors. The expectation in (10) amounts to a two-dimensional integration (over  $d_0$  and  $\theta_0$ ) of a series of error functions, where the series averages over the random set of interfering sectors,  $\mathcal{I}$ . We compute this expectation numerically.

On the uplink, we approximate the interference at the base station with an uplink noise rise parameter, defined as

$$\Lambda = \frac{P_I + P_N}{P_N}$$

where  $P_I$  is the total interference power from other sectors' UEs, and  $P_N = kTB10^{(F/10)}$  is the thermal noise power. Then, the uplink SINR is simply

$$\text{SINR}_{\text{ul}}(d, \theta, \Lambda) = \text{SNR}(d, \theta) - 10 \log_{10}(\Lambda) \quad (11)$$

and its cumulative distribution is evaluated by averaging the conditional distribution of (11) over the location of the UE in the sector.

#### D. Numerical Results

Figure 5 shows an example of uplink MCS probabilities in the urban environment with  $\sigma_s = 8$  dB shadowing and  $\Lambda = 6$  dB uplink noise rise. These probabilities were evaluated using SNR thresholds,  $\gamma_i$ , derived from the block error rate curves in the LTE module of OPNET Modeler [6]. More specifically,  $\gamma_i$  is the SNR that yields a  $10^{-3}$  block error rate using MCS  $i$ .

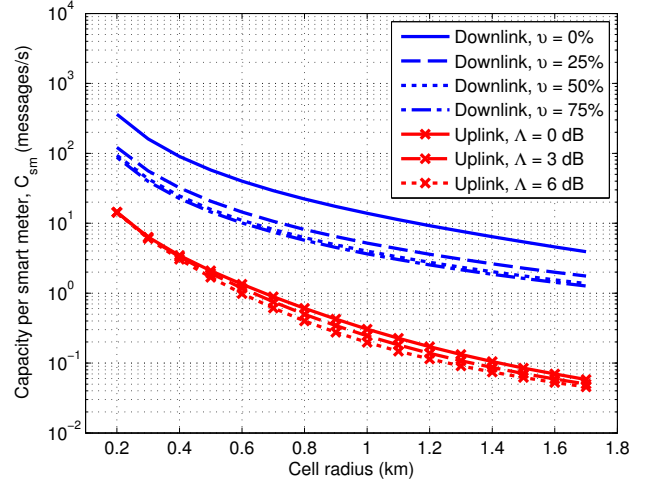


Fig. 6. Smart meter capacity in urban environment with 8 dB shadowing

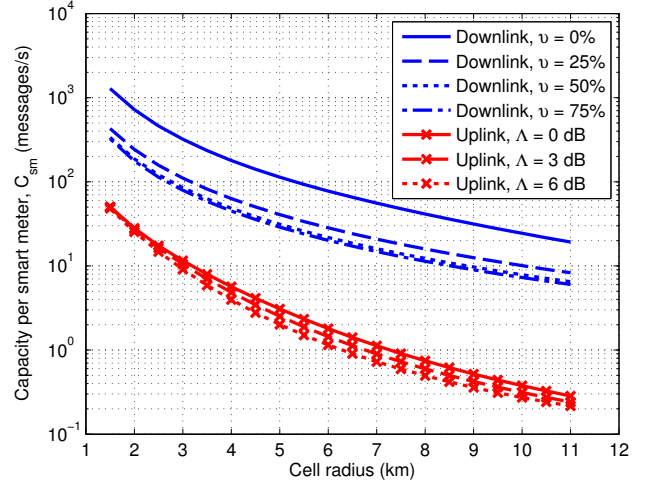


Fig. 7. Smart meter capacity in rural environment with 8 dB shadowing

Starting with MCS 0 at the bottom through MCS 28 on top, each band in the stacked plot of Fig. 5 represents the probability that an MCS is in use throughout a sector with that cell radius. As expected, with increasing cell size, the percentage of MCS 28 links decreases and those of lower-order MCSs increase, with moderate MCSs peaking at some intermediate cell radius. The overall coverage probability in the sector is given by the total of the MCS probabilities, which in this case is 0.78 at a cell radius of 1.7 km (before sector diversity).

Figures 6 and 7 plot the resulting capacity per smart meter,  $C_{\text{sm}}$ , versus cell radius,  $R_c$ , in the urban and rural environments, respectively. For the urban environment, we assumed a meter density of  $\rho_{\text{urban}} = 2000$  smart meters per  $\text{km}^2$ , while in the rural environment we assumed  $\rho_{\text{rural}} = 10$  smart meters per  $\text{km}^2$ .

In each figure, separate capacity curves are shown for downlink sector utilization levels of  $v = (0, 25, 50, 75) \%$ , and uplink noise rise values of  $\Lambda = (0, 3, 6)$  dB. In computing the

downlink MCS probabilities, the four sectors sharing an edge with the sector of interest comprised the superset from which the set of possible interferers,  $\mathcal{I}$ , was selected (i.e., sectors S1–S4 surrounding sector S0 in Fig. 2). Furthermore, the downlink utilization was used solely for assigning probabilities to the interference from neighboring sectors; the reported capacity in the sector of interest was not adjusted by this utilization. In other words, if all sectors had utilization  $v$  from other traffic, including the sector of interest, then the remaining capacity would be  $(1 - v) C_{\text{sm}}$ .

In general, smart meter capacity declines with cell size, due both to greater attenuation of the signal in the outer areas of the cell and to an increasing number of smart meters sharing sector resources. At the coverage limits of the respective environments, the results indicate maximum message rates on the downlink of 1–4 messages per second per meter in the urban environment and 6–20 messages per second per meter in the rural environment, depending on neighbor sector utilization. On the uplink, the maximum rates are near 0.05 messages per second per meter in the urban environment and 0.2–0.3 messages per second per meter in the rural environment at coverage limits. These capacity rates are orders of magnitude larger than the average rates for the meter reading and service switch use cases cited in Section II-A, implying that the WAN link is coverage-limited rather than capacity-limited and that excess capacity exists for other uses.

## V. CONCLUSION

We presented a framework to analytically study the performance characteristics and feasibility of a cellular WAN connecting metering headends to data aggregation points (or directly to smart meters) for advanced metering in a smart grid. The major components of the framework are a coverage analysis that predicts the maximum cell size subject to an outage criterion, and a capacity analysis that calculates the maximum long-term message rate per smart meter in the uplink and the downlink. Using the 3GPP LTE specification as an example of a cellular WAN, we used this framework to analyze the tradeoff between coverage and capacity, and to quantify the impact of variables like the propagation environment and sector utilization.

The results of the example analysis in the 700 MHz band suggest that metering traffic would initially utilize a small percentage of LTE resources and that the application would be coverage-limited rather than capacity-limited. Excess capacity would exist for additional application traffic and peak traffic conditions. Since even a highly loaded network would provide sufficient resources for metering, opportunities exist for sharing the WAN with other uses or with other entities. Extending coverage through repeaters or a multihop network would be another way to more efficiently utilize resources.

## REFERENCES

[1] J. A. Z. Torres, D. G. Arias, R. T. Miralles, and F. J. L. Perez, "Applicability of wireless communication technologies for measurement in the DENISE electrical distribution network," in *Proc. 20th Int'l Conf. on Electricity Distribution (CIRED)*, Jun. 2009.

[2] P. P. Parikh, M. G. Kanabar, and T. S. Sidhu, "Opportunities and challenges of wireless communication technologies for smart grid applications," in *Proc. IEEE PES General Meeting*, Jul. 2010.

[3] M. Souryal, C. Gentile, D. Griffith, D. Cypher, and N. Golmie, "A methodology to evaluate wireless technologies for the smart grid," in *Proc. IEEE SmartGridComm*, Oct. 2010, pp. 356–361.

[4] "Guidelines for assessing wireless standards for smart grid applications," NISTIR 7761, Jul. 2011.

[5] 3rd Generation Partnership Project Technical Report 36.942, "Radio frequency (RF) system scenarios," v. 8.2.0, Jun. 2009.

[6] "LTE PHY layer bit level simulations for modulation and coding curves," OPNET Design Document, Feb. 2010.